



NRC Publications Archive Archives des publications du CNRC

Validation of an open-source CFD tool to support efficient design of offshore gravity-based structures exposed to extreme waves

Babaei, Hossein; Baker, Scott; Cornett, Andrew

This publication could be one of several versions: author's original, accepted manuscript or the publisher's version. /
La version de cette publication peut être l'une des suivantes : la version prépublication de l'auteur, la version acceptée du manuscrit ou la version de l'éditeur.

Publisher's version / Version de l'éditeur:

Proceedings of the Twenty-seventh (2017) International Ocean and Polar Engineering Conference, pp. 662-669, 2017-06

NRC Publications Record / Notice d'Archives des publications de CNRC:

<https://nrc-publications.canada.ca/eng/view/object/?id=b9d83e08-0db7-4234-a336-394d26fa98e8>

<https://publications-cnrc.canada.ca/fra/voir/objet/?id=b9d83e08-0db7-4234-a336-394d26fa98e8>

Access and use of this website and the material on it are subject to the Terms and Conditions set forth at

<https://nrc-publications.canada.ca/eng/copyright>

READ THESE TERMS AND CONDITIONS CAREFULLY BEFORE USING THIS WEBSITE.

L'accès à ce site Web et l'utilisation de son contenu sont assujettis aux conditions présentées dans le site

<https://publications-cnrc.canada.ca/fra/droits>

LISEZ CES CONDITIONS ATTENTIVEMENT AVANT D'UTILISER CE SITE WEB.

Questions? Contact the NRC Publications Archive team at

PublicationsArchive-ArchivesPublications@nrc-cnrc.gc.ca. If you wish to email the authors directly, please see the first page of the publication for their contact information.

Vous avez des questions? Nous pouvons vous aider. Pour communiquer directement avec un auteur, consultez la première page de la revue dans laquelle son article a été publié afin de trouver ses coordonnées. Si vous n'arrivez pas à les repérer, communiquez avec nous à PublicationsArchive-ArchivesPublications@nrc-cnrc.gc.ca.



Validation of an Open-source CFD Tool to Support Efficient Design of Offshore Gravity-based Structures Exposed to Extreme Waves

Hossein Babaei, Scott Baker, Andrew Cornett

National Research Council Canada, Ottawa, Canada

ABSTRACT

Computational Fluid Dynamics (CFD) could be an inexpensive complement and even an alternative to physical modelling for investigating the interaction of ocean waves with offshore structures. CFD models however cannot be relied on unless they are well validated. We validated the OpenFOAM® CFD toolbox, a publically available open-source model, for modelling the interaction of extreme regular and irregular waves with offshore gravity-based structures. CFD results including water levels, pressures and forces generally compared well with results for a physical model test program previously conducted by the National Research Council Canada (NRC).

KEY WORDS: CFD; extreme regular waves; irregular waves; gravity-based structure; OpenFOAM; validation; IHFOAM; OLAFOAM.

INTRODUCTION

For optimal and safe design of offshore structures subjected to waves, accurate estimation of forces and water levels are needed. This estimation is usually obtained either by physical or numerical modelling approaches. Each approach has pros and cons: physical modelling usually involves smaller-than-reality model structures where the wave-structure interaction processes are subject to scale effects, and the study outputs are uncertain as a result. Physical modelling requires test facilities, model fabrication and instrumentation and hence can be expensive. Physical modelling however reveals many details of wave-structure interaction. Numerical modelling on the other hand is a relatively inexpensive approach without the model size limitation. If numerical models are based on correct physics and well validated, they are a reliable complement and perhaps even an alternative to physical modelling.

The literature on the validation of Computational Fluid Dynamics (CFD) models for studying wave-structure interaction is fast expanding and not fully developed. This is particularly true for the application of publically available open-source CFD models. Some of the most relevant recent literature is (Ong et al., 2017; Hu et al., 2016; Palomares, 2015; Chen et al., 2014; Paulsen et al., 2014; Palomón-

Arcos et al., 2014; Lambert, 2012; Thanyamanta et al., 2011; Afshar, 2010).

We have previously examined (Babaei et al., 2016) the applicability of the OpenFOAM CFD Toolbox, freely available and open source, for estimating the interaction of extreme regular waves with a four-column offshore gravity-based structure. Therein, it was shown that OpenFOAM results are very similar to results of an equivalent physical model test program conducted previously at the National Research Council Canada (NRC). A summary of the physical model test program is given in the next section.

The present paper describes further validation of OpenFOAM and focuses on two test cases in which the interaction of highly nonlinear waves with a fixed structure similar to the four-column structure from (Babaei et al., 2016) is simulated and assessed. In one case, a marginally unstable regular wave condition associated with a 10,000-year event is studied, while a long-crested irregular wave condition associated with a 100-year event is considered in the second case.

SUMMARY OF THE PHYSICAL MODEL STUDY

NRC has previously conducted a series of physical hydraulic model tests (Cornett, 2011) to assist in designing an offshore liquefied natural gas processing platform to resist extreme waves expected for the deployment site. Tests were conducted at a length scale of 1:50 in NRC's 36 m wide by 30 m long by up to 3 m deep Multidirectional Wave Basin located in Ottawa, Canada. Froude scaling was used to convert measured quantities (including wave height, pressure, and force) to full scale values. The 1:50 scale was selected to ensure that the required wave conditions could be generated in the basin and to minimize scale effects related to improper scaling of surface tension and water viscosity.

The model platform sub-structure (SS) and the lowest parts of the deck structure was designed and fabricated by NRC and several sub-contractors. The model was instrumented to measure many quantities, including water surface elevations and run-ups at twenty two locations; water velocity at four locations; global forces on the entire model; global forces on the deck structure; hydrodynamic forces on each deck post; hydrodynamic forces on wave deflectors mounted near the top of the SS columns; hydrodynamic forces on wave deflectors mounted near the top of the deck posts; hydrodynamic forces on a horizontal test

beam suspended below the deck structure; local hydrodynamic pressures caused by intermittent water contact at twenty eight locations on the surface of the SS columns; and hydrodynamic uplift pressures because of intermittent water contact at eighteen locations on the underside of the deck structure. All sensor outputs were collected at sampling rates ranging from 50 Hz to 10 kHz using a pair of synchronized data acquisition systems. Five video cameras recorded all tests, including a high-speed 500 frames per second digital video camera.

The model platform was tested in several different configurations: SS alone; SS with a grated (porous) deck structure, SS with a plated (non-porous) deck structure; SS with a plated deck structure and wave deflectors at the top of each column; SS with a plated deck structure and an enhanced sub-cellar deck; and SS with a plated deck structure, an enhanced sub-cellar deck, and small wave deflectors on the deck support posts. For each configuration, tests were conducted in extreme wave conditions associated with return periods of 100, 1,000, and 10,000-years. Figure 1 shows a photo of wave run-up impacting the underside of the deck structure taken during one of the tests. The model was tested with regular waves, long-crested irregular waves with 3-hour duration, short-crested irregular waves with 3-hour duration, and short-crested and long-crested wave snapshots (relatively brief periods of irregular wave activity selected to contain at least one extreme wave). The model was mounted on a concrete turntable, and three different wave headings (0° , 33° , and 90°) were simulated by rotating the model within the wave basin.

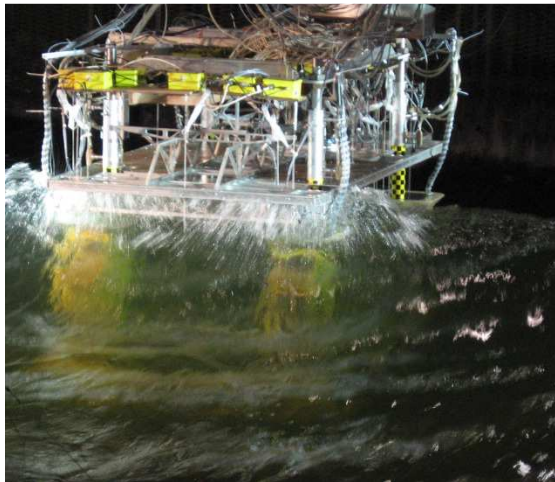


Fig. 1. A snapshot of the interaction of an extreme wave with the structure from the physical model test.

STRUCTURE GEOMETRY AND WAVE CONDITIONS

Figure 2 shows the two structure configurations modelled in the present paper, named config A and config C. The difference between the two configurations is that the C config includes a large horizontal plated solid deck, risers on both front columns and a small grated (screen) sub-cellar deck.

Figure 2 also shows two CAD models representing the two configurations in the present CFD study. The two CAD models are simplifications of the physical model configurations to reduce the computational time of the present CFD modelling; cross and vertical braces were neglected based on a CFD sensitivity study proving that the braces do not notably impact the hydrodynamics. The horizontal braces which are the thickest and longest braces were however modelled in the CAD, although the horizontal braces also do not impact

the hydrodynamics. The grated (screen) small sub-cellar deck was neglected. This decision was based on comparing maximum uplift (vertical) forces exerted by waves for two different model configurations: one without any deck structure and the other with a large horizontal grated (porous) deck. The uplift forces were very similar suggesting that the existence of a grated sub-cellar deck could be neglected, at least for the estimation of uplift forces. The impact of risers on hydrodynamics was also assumed to be negligible.

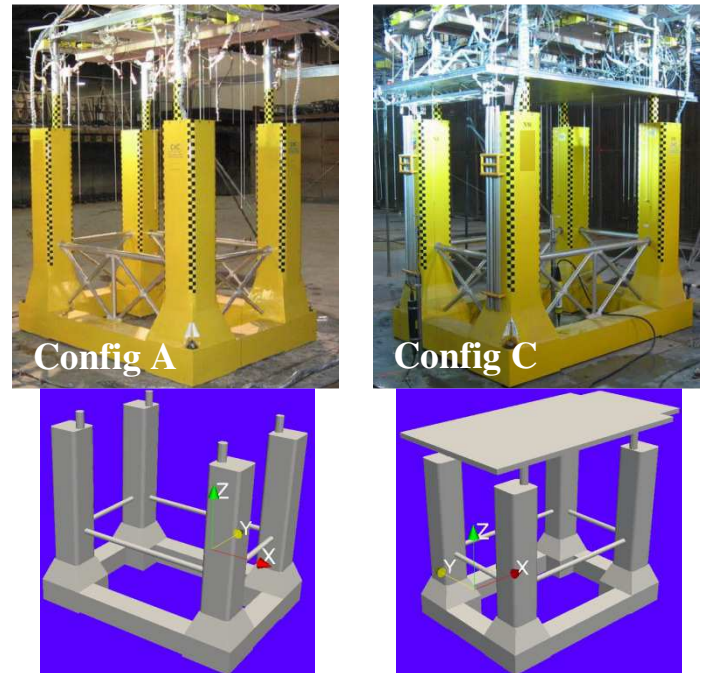


Fig. 2. Physical model configurations and their CAD model counterparts: Top left: config A, top right: config C, bottom left: CAD model for config A, bottom right: CAD model for config C. Blender and netfabb Basic computer tools were used for the CAD modelling and improvements.

The dimensions (along X, Y, and Z directions shown in Fig. 2) of the bounding box of config A and C are respectively 2.06 m by 1.50 m by 1.88 m, and 2.53 m by 1.51 m by 2.01 m.

Two cases were modelled numerically: Case 1 – the interaction of regular waves with config C; and Case 2 – the interaction of long-crested irregular waves with config A. Table 1 lists more information about the two cases. For both cases the incident waves propagate in the +X direction.

Table 1. Two cases modelled in the present paper

	Config	Calm water depth, m	Wave height, m	Wave period, s
Case 1	C	1.454	0.776	2.404
Case 2	A		Irregular	

The regular wave condition for Case 1 is associated with a relative depth (wave height/calm water depth) of 0.534 which is very close to the experimental limit of depth-limited wave breaking for regular waves which is 0.55 (Riedel and Byrne, 1986). Although the regular waves did not break during the physical test program, some minor spilling at the wave crest was observed.

The irregular wave snapshot for Case 2 was associated with a 100-year event. The actual paddle motions from the physical model study were used to numerically generate the irregular wave condition for the present paper, a portion of this time-series was imposed at the “upstream” boundary of the numerical wave tank. This time-series of paddle motions is given in Fig. 3. More information about the numerical generation of irregular waves is given later in the paper.

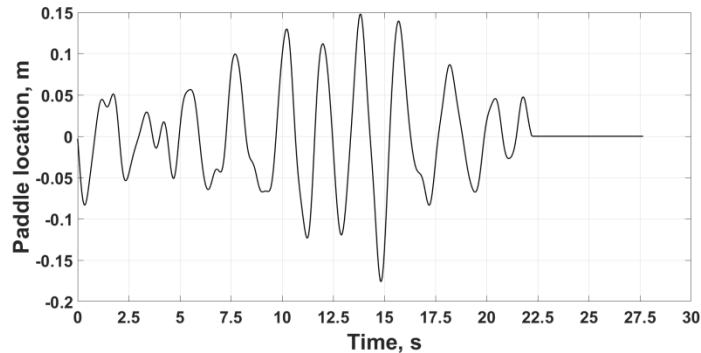


Fig. 3. Time-series of the horizontal location of paddles generating the irregular long-crested waves for Case 2.

GOVERNING EQUATIONS AND OpenFOAM SOLVER

The present problem is a fluid dynamics problem involving two phases (air and water). Two laws of physics relevant to this problem are the conservation of mass and momentum formulated by Navier-Stokes equations which for an incompressible Newtonian fluid with a constant viscosity read as follows:

$$\nabla \cdot \mathbf{u} = 0 \quad (1)$$

$$\frac{\partial \rho \mathbf{u}}{\partial t} + \nabla \cdot (\rho \mathbf{u}) \mathbf{u}^T = -\nabla p^* - (\mathbf{g} \cdot \mathbf{x}) \nabla \rho + \nabla \cdot (\mu \nabla \mathbf{u}) + \mathbf{S} \quad (2)$$

where \mathbf{u} , ρ , p^* , \mathbf{g} , μ and \mathbf{S} are respectively velocity vector, density, pseudo-dynamic pressure ($= p - \rho \mathbf{g} \cdot \mathbf{x}$), gravity vector, viscosity and other body forces vector, and p is the total pressure. ∇ , \cdot , ∂ , superscript T, t and \mathbf{x} respectively denote the del operator, the dot product, partial derivative, matrix transpose, time, and location vector.

OpenFOAM (version 2.2.2), a publically available open-source general purpose CFD toolbox, was selected for the present study. OpenFOAM is capable of modelling several different physics including compressible and incompressible, and single and multiphase flow dynamics with a powerful body-fitting meshing utility. OpenFOAM’s main discretization method is finite-volume.

Additional developments to OpenFOAM to generate and absorb waves have been on the Volume of Fluid (VOF) two-phase flow solver of OpenFOAM. VOF is an interface capturing method. To track the interface between the phases, an advection equation is added to the governing equations given by Eq. 1 and Eq. 2, as follows:

$$\frac{\partial \alpha}{\partial t} + \nabla \cdot \mathbf{u} \alpha + \nabla \cdot \mathbf{u}_c \alpha (1 - \alpha) = 0 \quad (3)$$

where α is a phase identifier. In the present study α is 1 for water, and 0 for air, and an intermediate value in the interface region. This equation is then only applicable to the interface region. The third term in the left-hand side of the above equation is not needed for the theoretical representation of the interface and is only added for the numerical stability and the conservation of a sharp interface. \mathbf{u}_c is

$\min(c_\alpha |u|, \max |u|)$ and c_α is a constant usually between 0 and 1 assigned by CFD modelers. c_α is 2 for Case 1, and 1 for Case 2 in the present study.

In the VOF method, two phases are represented with a single fluid whose density and viscosity is a function of α :

$$\begin{aligned} \rho &= \rho_w \alpha + (1 - \alpha) \rho_a \\ \mu &= \mu_w \alpha + (1 - \alpha) \mu_a \end{aligned} \quad (4)$$

and then only one set of Navier-Stokes equations is solved.

For the generation and the active absorption of numerical waves, IHFOAM (Higuera et al., 2013) (for Case 1) and OLAFOAM, an evolution of IH-FOAM, (for Case 2) were employed. Other wave models developed for use with OpenFOAM include groovyBC and waves2foam (Jacobsen et al., 2012); however they were not assessed in the present CFD study.

MODEL DETAILS AND NUMERICAL WAVE TANK

Boundary Conditions

Boundary conditions are identical to the condition explained in (Babaei et al., 2016) except for Case 2, the irregular wave case, where some conditions are added to impose the horizontal motion of the numerical wave tank’s “upstream” boundary for the generation of irregular waves. Because of the symmetry of waves and configurations, shown in Fig. 2, only half of the structure is modelled by imposing symmetry on one of the tank’s walls.

Turbulent vs Laminar Modelling

The present problem for both cases involves turbulent flows. We attempted to model the turbulence by OpenFOAM’s $k - \epsilon$ turbulence model. Standard settings of the turbulence model led to unrealistically large wave dissipations. We did not seek reasons of large dissipations and did not investigate other turbulence models available in OpenFOAM® and modelled flows for both cases as laminar flows.

Geometry of the Numerical Tank

The numerical tank is a rectangular block whose vertical dimension is just enough to prevent water to reach the top boundary plane. Therefore, the height of the tank for Case 1 is different from that of Case 2. For Case 1, the length of the tank along the direction of incoming waves (X direction) is 16.5 m which is approximately two wavelengths. For Case 2, because of the irregularity of waves, the structure must have been located at the same distance from the “upstream” paddles in the numerical tank as it was in the physical test program. The center of the structure is thus 14.36 m away from paddles. Enough space was given “downstream” of the structure for Case 2 to prevent possible waves reflected from the “downstream” boundary to reach the structure. The total size of the tank along the X axis for Case 2 is 43.08 m. The size of the tank along the Y axis was decided based on our available computational “budget”; for Case 1 it is 3.52 m and for Case 2 it is 2.52 m.

Model Mesh and Computational Time

The mesh cells are cubical (equilateral) away from the structure and hexahedral and split hexahedral (to conform to the structure) as one approaches the structure. *BlockMesh* and *SnappyHexMesh* utilities of OpenFOAM were used for meshing. The cubical cell size for Case 1 is

0.052 m representing the wave height by approximately 15 cells. The cubical cell size for Case 2 is 0.036 m representing the largest wave by approximately 12 cells. Mesh is not refined at the water-air interface. The total number of cells for Case 1 and Case 2 are approximately 0.97 M and 4.9 M, respectively. Shared Services Canada's Vulcan cluster was used for computations. Case 1 was run on 50 parallel processors and each wave period took approximately 1.8 days to compute. Case 2 was run on 90 processors and 27.5 s of physical time took approximately 9 days to compute. Computational time step size changes automatically during both simulation cases to satisfy accuracy and convergence conditions. For both cases, typical order of magnitude of time step size is 10^{-4} s.

RESULTS

Case 1 Results

Waves for this case were regular long-crested with height and period as given in Table 1. Based on the wave theory chart by Le Mehaute (1976), Stokes IV is the most suitable wave theory for this case. 5th order stream function and cnoidal theories are also suitable.

We first investigated how waves propagate and evolve with time and location in the numerical tank in the absence of the structure. We attempted to generate waves based on three different wave theories separately: Stokes V, 5th order stream function theory, and cnoidal theories provided by IHFOAM. For the 5th order stream function wave generation a calculation, based on (Fenton, 1990), was required prior to the numerical wave generation by IHFOAM. When the wave condition for this case, given in Table 1, is input to the CFD model, generated waves become unrealistically unstable and break after a short distance. This instability is regardless of the wave theory used. Instability of waves modelled by OpenFOAM's VOF solver have been previously attributed to incorrectly high estimations of air speeds at air-water interface for steep waves (Afshar, 2010). Wave steepness (wave height/wavelength) for the present case is approximately 0.095. For the present case we used Stokes V theory and reduced the input wave height by 15% to reproduce target waves.

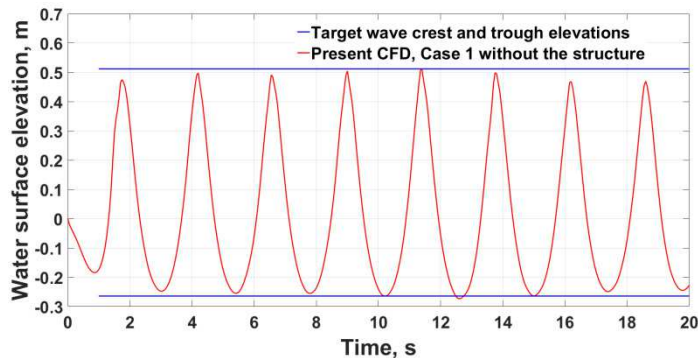


Fig. 4. Modelled waves satisfy target trough and crest elevations for Case 1. Time-series of modelled regular waves ~ 1.1 m “downstream” of the wave-generating boundary.

After successfully reproducing the highly nonlinear regular waves in the numerical tank, Fig. 4, the interaction of waves with the structure, config C shown in Fig. 2, was modelled. To avoid the interaction of undesirably evolved waves as they propagate in the domain, as discussed above, the center of the structure was positioned approximately 3.3 m “downstream” of the wave-generating plane. (In the physical model study the model structure was located further away from the wave generator.) Local velocities, air gaps, run-ups, local

pressures, global forces, and the main overturning moment were compared with measured values. Figure 5 shows locations and names of water level, local pressure, and speed probes referred to in following figures of the present subsection.

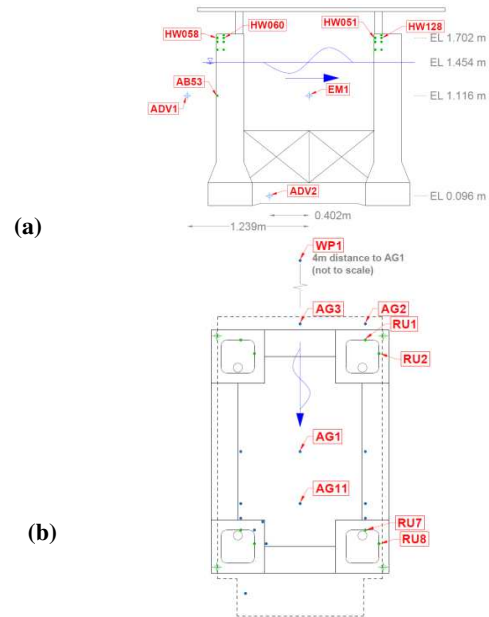


Fig. 5. Locations and names of sensors. (a) local pressures on the structure and flow speeds, (b) water surface elevations

The present CFD model correctly predicts the X component of the flow at three different locations, Fig. 6. This correct estimation shows that the reduction in the input wave height to prevent the breaking of waves did not compromise the velocity field. Note that all velocity probes are on the symmetry plane perpendicular to Y axis.

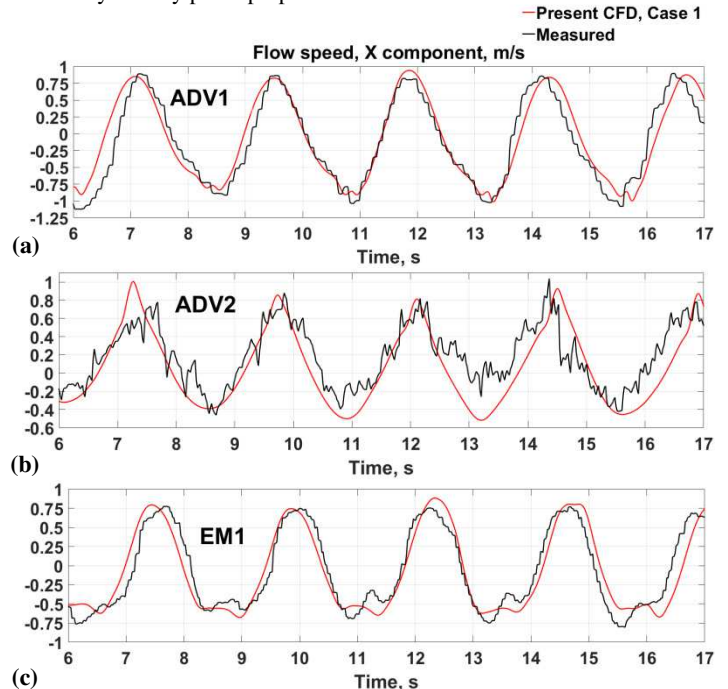


Fig. 6. Modelled speeds are consistent with measurements. The X component of velocity at three different locations shown in Fig. 5a.

Modelled air gaps were compared with corresponding measurements at several different locations. Results were very consistent with measurements, Fig. 7. Physically generated waves have slightly smaller period than the target wave period. This is the main reason why the time values associated with the extremums of most of the modelled quantities do not match those of the measured.

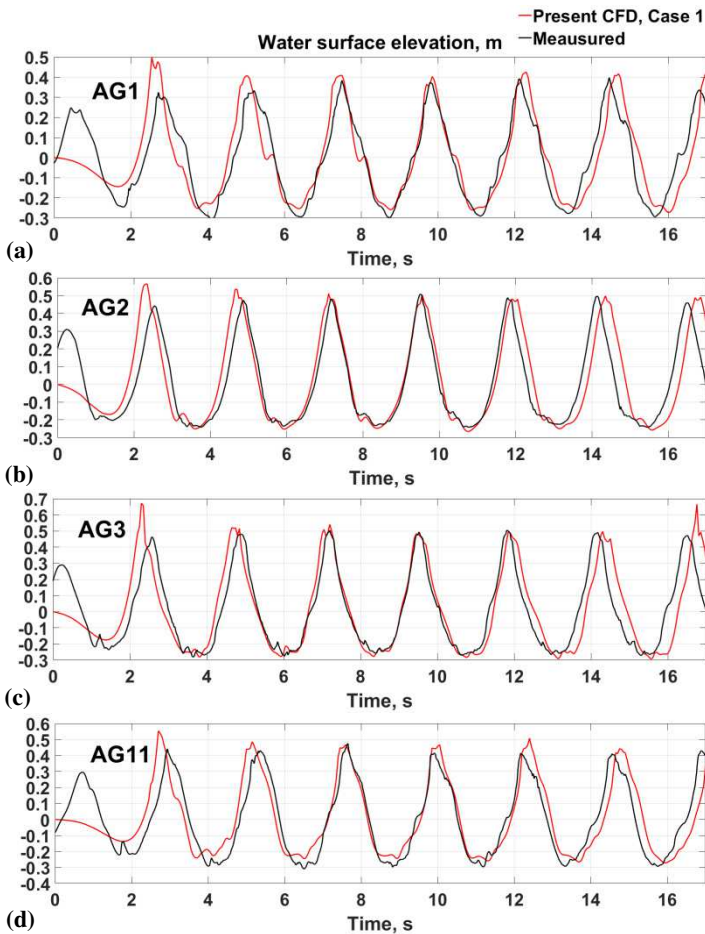


Fig. 7. Modelled air gaps are consistent with measurements.

Modelled run-ups are also generally correctly estimated, Fig. 8. Note that waves for the present case are high enough to interact with the large horizontal plated solid deck whose lower surface is approximately 0.51 m above the calm water level.

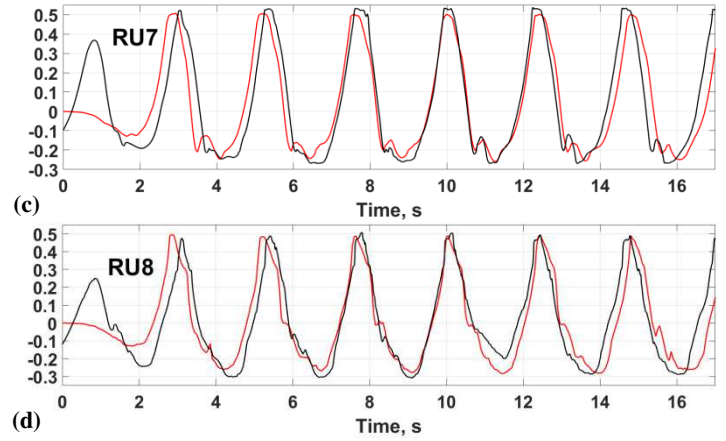
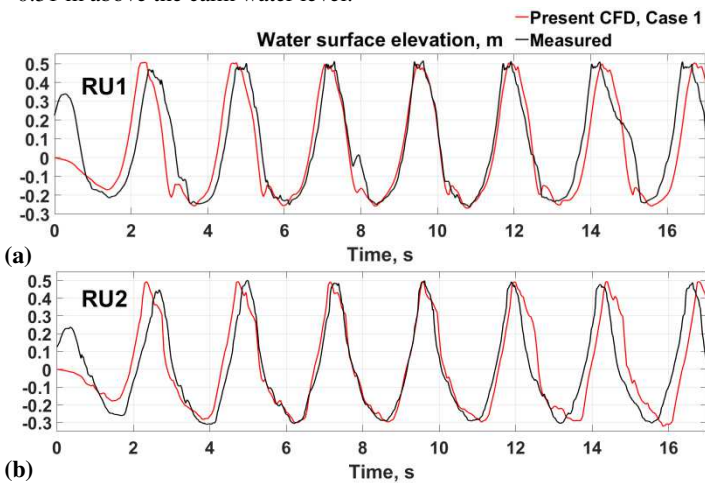
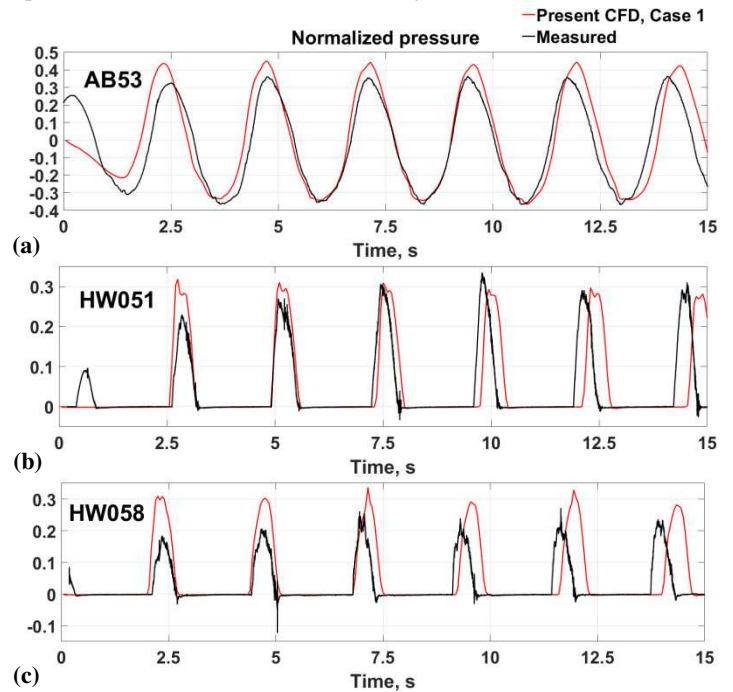


Fig. 8. Modelled run-ups are generally consistent with measurements.

Peak values of modelled local pressures on columns tend to be generally slightly larger than the measured values. This is true for both the underwater sensor, AB53, and other pressure sensors located above the still waterline. In the physical model study, the underside of the top deck had been instrumented with several local pressure sensors. Modelled pressures for some of those sensors were compared with measurements; however, the present model results were not consistent with measurements. Impacts on the underside of the deck are extremely complex and stochastic, and even the physical model had issues of repeatability of impact events during duplicated tests. The output frequency of the present CFD model results had been set to 20/s, which is not enough to resolve the impact-like behavior of local pressures for some of locations under the deck. Whether increasing the output frequency of the CFD model improves the estimation of the local pressures under the deck was not investigated.



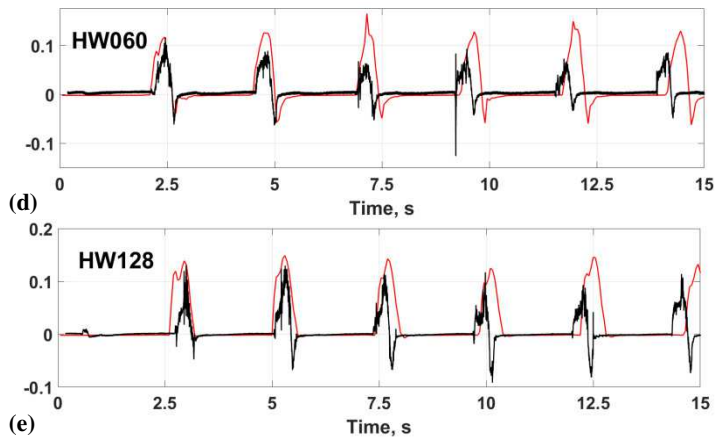


Fig. 9. Modelled local pressures are higher than measurements for some of wave cycles except for the underwater sensor AB53 where modelled peak values are slightly larger for all wave cycles.

Global X and the dynamic Z components of the force, and the Y component of the overturning moment are also consistent with measurements, Fig. 10. The X component, in-line with the propagation direction of waves, is very well predicted, Fig. 10a. The dynamic Z component of the force shows two local peaks, associated with the impact of run-ups with the top deck; the existence of these peaks are correctly predicted by the present CFD model although the peak values are generally slightly underpredicted, Fig. 10b, which may also be a result of the CFD model output frequency being too small, as mentioned earlier. The Y component of the overturning moment is almost equally influenced by errors in the X and the Z components of the force, considering the length of the moment arm. Nevertheless, the modelled overturning moment is consistent with measurements, particularly for the peak values, Fig. 10c.

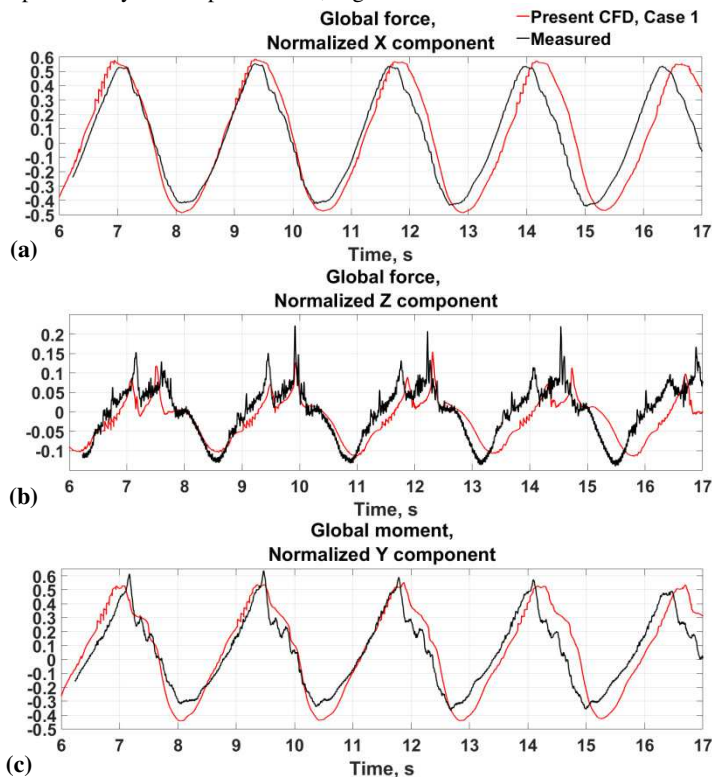


Fig. 10. Modelled global forces and the overturning moment are consistent with measurements.

Case 2 Results

This case featured an irregular long-crested wave snapshot. Generation of the numerical waves was based on the actual paddle motions, Fig. 3, from the physical model.

Unlike Case 1 where waves were generated at a stationary boundary, for Case 2 waves were generated by the horizontal motion of the boundary similar to the physical test program. For this wave generation and active wave absorption, we used OLAFOAM which is based on the dynamic mesh VOF solver of OpenFOAM. In this subsection we have briefly studied the applicability of OLAFOAM for the reproduction of the physical test results for the irregular wave condition.

It is known that the mesh cell size impacts the numerical diffusion, an unwanted behavior of most of mesh-based CFD models. This diffusion could lead to the damping of waves propagating in a numerical tank. In the context of the mesh-based CFD modeling of waves, it is generally recommended to discretize wave heights by at least 10 to 15 cells, and wavelengths by at least 70 cells. For the present Case 2 involving irregular waves with heights ranging approximately from 0.05 m to 0.5 m, this recommendation cannot be followed for the smaller waves because computational time will be unpractically large.

We studied the applicability of OLAFOAM for irregular wave generation in the basin in the absence of the structure and also the effect of cell size on modelled waves. Two cell sizes were considered: a cubical 3D cell size of 0.0364 m and a square 2D cell size of 0.0145 m. The latter cell size could not be practically modelled in 3D because of very large computational time.

Modelled waves at three different locations were compared with measurements from the physical model study. Modelled waves have generally similar trends to those of measurements. Particularly, the largest wave is very well reproduced. Results of the coarse 3D model do not significantly differ from those of the fine 2D model. This confirms that results are not considerably mesh dependent from the course mesh to the fine mesh considered here. Whether further mesh refinements improve model results was not investigated. Differences between modelled and measured results could have different reasons. OLAFOAM does not accept paddle speed time-series as input to generate irregular waves; it only accepts paddle location time-series. The speed of the moving boundary is then based on time-series of paddle locations which leads to speed discontinuity. This discontinuity could be a source of inaccuracy. This issue requires further investigation. Wave paddles in the physical basin were driven by hydraulics actuators known to have a delayed response depending on required displacements. Whether the actual time-series of the physical motion of the paddles matches the target, shown in Fig. 3, is unknown to the authors. Reflection of particularly long waves from boundaries of the physical basin could have also degraded the target wave generation. Heights of reflected physical waves are estimated to be up to 10% of those of incoming waves for this case.

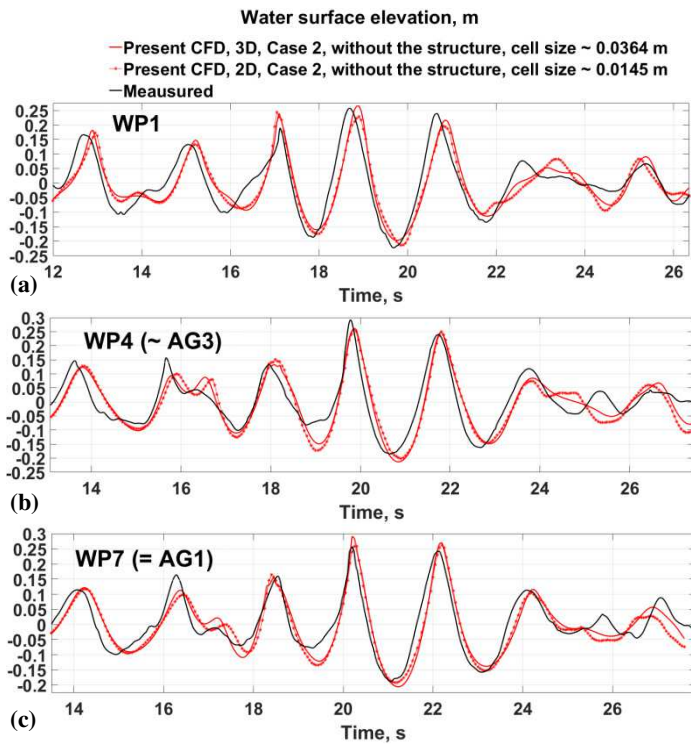


Fig. 11. Modelled irregular waves are generally consistent with measured waves, particularly for the largest wave, passing through three different locations.

After the satisfactory generation of waves in the tank, the interaction of waves with the structure, config A shown in Fig. 2, was briefly studied. Figure 12 shows that modelled air gaps and run-ups are generally consistent with measurements. Despite several attempts including model re-run and the application of different post-processing interpolation algorithms, results for AG3, RU1 and RU7 could not be obtained. This was because of a problem related to the OpenFOAM's post-processing of CFD results.

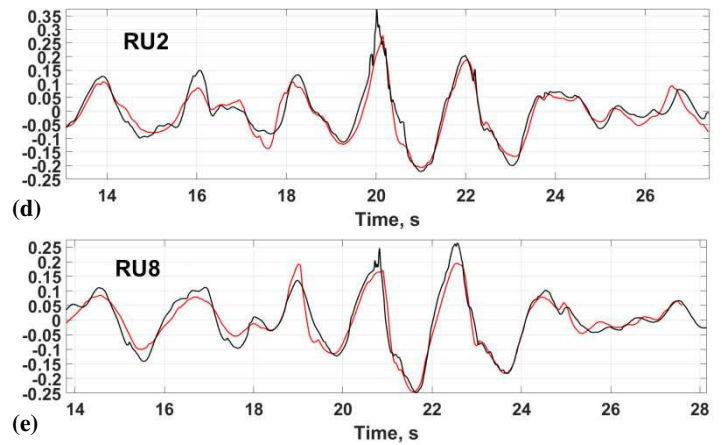
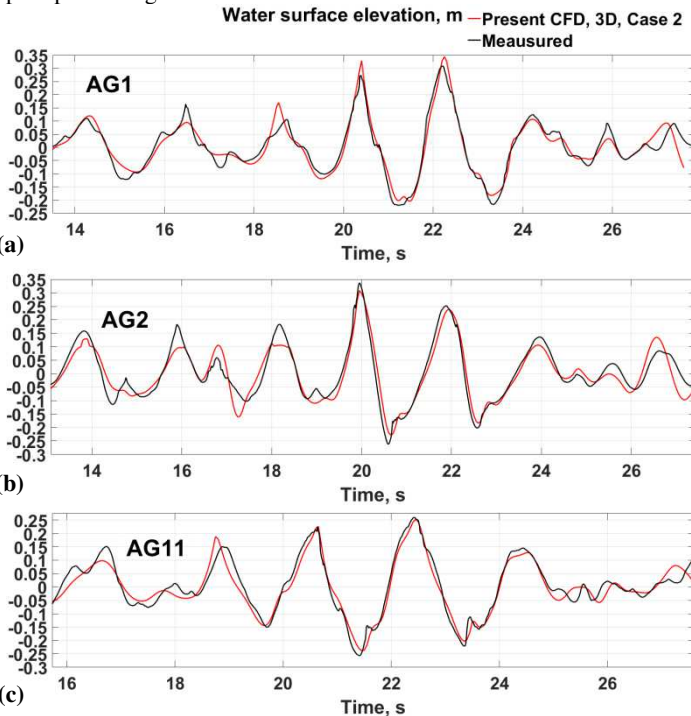


Fig. 12. Modelled air gaps and run-ups are generally consistent with measurements.

Local maximums of modelled in-line (X direction) global forces are consistent with measurements; however, local minimums are generally slightly underpredicted, see Fig. 13a. The modelled dynamic Z component (vertical) of the global force is generally not consistent with measurements, although general trends are similar, see Fig. 13b. It is noted that the vertical forces are an order of magnitude smaller than the horizontal forces for this case. In a previous study (Babaei et al., 2016) of the same structure, config A, the vertical global force was found to be sensitive to the size of the small gap separating the structure from the tank bottom. This gap was needed in the physical model to isolate the structure from the ground to correctly measure wave forces. We are not certain whether the gap size assumed in the present modelling is the same as in the experiments. This uncertainty could be a source of the general inconsistency in vertical forces. Another possible reason could be flaws in the physical load sensors. Further investigations are required to confirm or disprove these hypotheses.

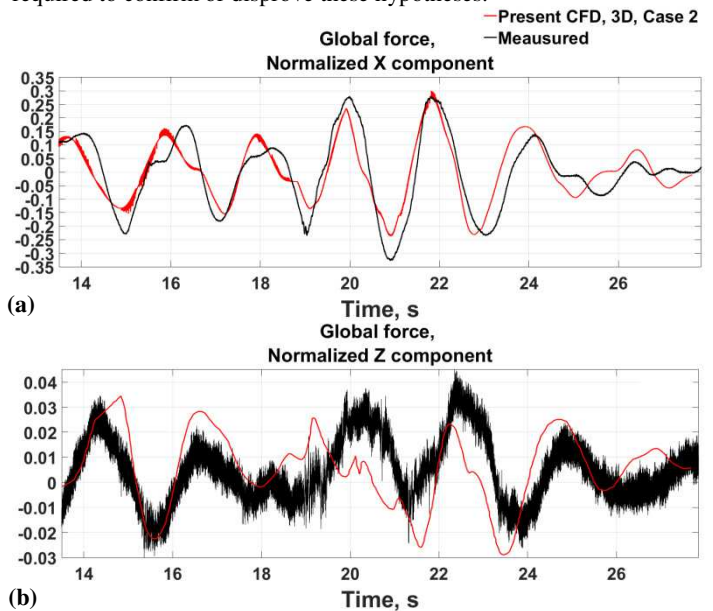


Fig. 13. The modelled global in-line is generally consistent with measurements, but the global vertical force is not.

CONCLUSIONS AND FUTURE WORK

The validity of the free open-source OpenFOAM CFD Toolbox for conducting simulations of the interaction of highly nonlinear waves with two similar four-column gravity-based rigid structures was studied. Two extreme long-crested wave conditions were modelled: a near-breaking regular wave and an irregular wave snapshot. Model results including water surface elevations and global forces were compared with results of a previous physical model study conducted at the National Research Council Canada. Results for both wave conditions alone and the wave-structure interaction were generally consistent with measurements. This consistency confirms the dependability of OpenFOAM and the other two used models, OLAFOAM and IHFOAM, built on OpenFOAM, for the generation, absorption and interaction of investigated wave types with fixed structures.

Future efforts could focus on: (1) the inclusion of turbulence in the modelling and investigating how and if this could improve CFD results, (2) investigating the reason for the disagreement between the modelled and measured pressures acting on the underside of the horizontal deck subjected to wave impacts, (3) investigating whether and how extreme mesh refinements improve the estimation of smaller waves for the irregular wave case.

ACKNOWLEDGEMENTS

The authors thank Pablo Higuera with the National University of Singapore for his help with the capabilities of IHFOAM and OLAFOAM, Dan Pelletier with the National Research Council Canada for providing the irregular paddle motion time-series and general insights about wave generation and absorption in the physical test basin, and the National Research Council Canada for financial support.

REFERENCES

- Afshar, MA (2010). *Numerical Wave Generation in OpenFOAM®*, Master's thesis, Chalmers University of Technology, Goteborg, Sweden.
- Babaei, H, Baker, S, and Cornett, A (2016). "Validation of a CFD Tool for Studying the Interaction of Extreme Waves with Offshore Gravity-based Structures", *Proceedings of the 6th International Conference on the Application of Physical Modelling in Coastal and Port Engineering and Science (Coastlab16)*, Ottawa, 1-11.
- Chen, LF, Zang, L, Hillis AJ, Morgan JCJ, and Plummer, AR (2014). "Numerical Investigation of Wave-structure Interaction Using OpenFOAM", *Ocean Engineering*, 88, 91-109.
- Cornett, A (2011). *Hydraulics Model Studies of Extreme Wave Interaction with the Wheatstone Platform*, Canadian Hydraulics Center, Report ID: CHC-CTR-0120.
- Fenton, JD (1990). "Nonlinear Wave Theories", *The Sea (9): Ocean Engineering Science*, Eds. Le Méhauté, B, and Hanes, DM, Wiley, New York.
- Higuera, P, Lara, JL, and Losada, IJ (2013). "Realistic Wave Generation and Active Wave Absorption for Navier-Stokes Models Application of OpenFOAM®", *Coastal Engineering*, 71, 102-118.
- Hu, ZZ, Greaves, D, and Raby A (2016). "Numerical Wave Tank Study of Extreme Waves and Wave-structure Interaction Using OpenFOAM®", *Ocean Engineering*, 126, 329-342.
- Jacobsen, NG, Fuhrman, DR, and Fredso, J (2012). "A Wave Generation Toolbox for the Open-source CFD Library: OpenFOAM®", *International Journal of Numerical Methods in Fluids*, 70(9), 1073-1088.
- Lambert, RJ (2012). *Development of a Numerical Wave Tank Using*

- OpenFOAM*, Master's thesis, Coimbra University, Coimbra, Portugal.
- Le Méhauté, B (1976). *An Introduction to Hydrodynamics and Water Waves*, Springer-Verlag, New York.
- Ong, MC, Kamath A, Bihs, H, and Afzal, MS (2017). "Numerical Simulation of Free-surface Waves Past Two Semi-submerged Horizontal Circular Cylinders in Tandem", *Marine Structures*, 52, 1-14.
- Palemón-Arcos, L, Torres-Freyermuth, L, Chang, K, Pastrana-Maldonado, D, and Salles, P (2014). "Modeling Wave-structure Interaction and its Implications in Offshore Structure Stability", *Proc 24th International Ocean and Polar Engineering Conf*, Busan, ISOPE, (2) 613-617.
- Palomares, GD (2015). *CFD Simulations on a Partially Submerged Cylinder under Regular Waves Using OPENFOAM®*, Master's thesis, University of Stavanger, Norway.
- Paulsen, BT, Bredmose, H, Bingham, HB, and Jacobsen, NG (2014). "Forcing of a Bottom-mounted Circular Cylinder by Steep Regular Water Waves at Finite Depth", *Journal of Fluid Mechanics*, 555, 1-34.
- Riedel, HP, and Byrne, AP (1986). "Random Breaking Waves – Horizontal Seabed", *Coastal Engineering*, 903 – 908.
- Thanyamanta, W, Herrington, P, and Molyneux, D (2011). "Wave Patterns, Wave Induced Forces and Moments for a Gravity Based Structure using CFD", *International Conference on Ocean, Offshore and Arctic Engineering*, Rotterdam, 1-11.